Development 133, 1389-1398 (2006) doi:10.1242/dev.02294

PAR3 is essential for cyst-mediated epicardial development by establishing apical cortical domains

Tomonori Hirose[1,2,3], Mika Karasawa[3], Yoshinobu Sugitani[3], Masayoshi Fujisawa[3], Kazunori Akimoto[1], Shigeo Ohno[1,*] and Tetsuo Noda[3,4,5]

Epithelial cysts are one of the fundamental architectures for mammalian organogenesis. Although in vitro studies using cultured epithelial cells have revealed proteins required for cyst formation, the mechanisms that orchestrate the functions of these proteins in vivo remain to be clarified. We show that the targeted disruption of the mouse *Par3* gene results in midgestational embryonic lethality with defective epicardial development. The epicardium is mainly derived from epicardial cysts and essential for cardiomyocyte proliferation during cardiac morphogenesis. PAR3-deficient epicardial progenitor (EPP) cells do not form cell cysts and show defects in the establishment of apical cortical domains, but not in basolateral domains. In PAR3-deficient EPP cells, the localizations of aPKC, PAR6β and ezrin to the apical cortical domains are disturbed. By contrast, ZO1 and α4/β1 integrins normally localize to cell-cell junctions and basal domains, respectively. Our observations indicate that EPP cell cyst formation requires PAR3 to interpret the polarity cues from cell-cell and cell-extracellular matrix interactions so that each EPP cell establishes apical cortical domains. These results also provide a clear example of the proper organization of epithelial tissues through the regulation of individual cell polarity.

KEY WORDS: PAR3 (PARD3), Gene targeting, Epithelial cell polarity, Epithelial cyst, Heart development, Epicardium, Mouse

INTRODUCTION

The organization of polarized epithelial cells is crucial for ontogeny and function of various tissues and organs in metazoans (Rodriguez-Boulan and Nelson, 1989). An epithelial cyst is one of the simplest architectures with organized epithelial cells (O'Brien et al., 2002). During embryonic development in mammals, epithelial cysts serve as progenitors for the morphogenesis of more complex organs, for example, blastocysts, somites, cysts of epicardial progenitor (EPP) cells and renal vesicles (Gumbiner, 1996; Manner et al., 2001). Epithelial cysts are composed of monolayers of polarized epithelial cells surrounded by or enclosing extracellular matrices (ECMs). Epithelial cells in completely developed cysts establish cell-cell junctions and the polarized compartmentation of cortical subdomains: the apical domain facing the lumen and the basolateral domain adhering to ECM (O'Brien et al., 2002). Cadherin-mediated cell-cell contacts and integrin-mediated contacts to ECM, particularly to basement membrane laminins, provide the spatial cues for epithelial cell polarity (Drubin and Nelson, 1996; Gumbiner, 1996; Li et al., 2003; Rodriguez-Boulan and Nelson, 1989). Results obtained from targeted gene disruption studies and Madin-Darby Canine Kidney (MDCK) cyst formation assay indicate that laminin-mediated signaling through integrin-linked kinase and Rac1 small GTPase are involved in epithelial cyst development (O'Brien et al., 2001; Sakai et al., 2003). However, the hierarchy of signaling pathways in the development of epithelial cysts remains to be clarified.

[1]Department of Molecular Biology, Yokohama City University Graduate School of Medical Science, Yokohama 236-0004, Japan. [2]Kihara Memorial Yokohama Foundation for the Advancement of Life Sciences, Yokohama 244-0813, Japan. [3]Department of Cell Biology, JFCR-Cancer Institute, Tokyo 135-8550, Japan. [4]Center for Translational and Advanced Animal Research (CTAAR), Tohoku University School of Medicine, Sendai 980-8575, Japan. [5]CREST, Japan Science and Technology Corporation (JST), Saitama 332-0012, Japan.

*Author for correspondence (e-mail: ohnos@med.yokohama-cu.ac.jp)

Accepted 19 January 2006

Accumulating experimental evidence suggests that the mammalian homologs of *Caenorhabditis elegans* polarity proteins, including PAR3 (PARD3 – Mouse Genome Informatics), have evolutionarily conserved functions in the establishment of cell polarity in various cell types (Macara, 2004; Ohno, 2001). PAR3 contains one self-oligomerization domain in the N terminus, three PDZ protein interaction domains and one aPKC-binding domain (Izumi et al., 1998; Mizuno et al., 2003). PAR3 forms a conserved protein complex with PAR6 and aPKC, and these three proteins are interdependent in their normal distribution in the mammalian epithelia (Joberty et al., 2000; Suzuki et al., 2001). The analyses of the polarity of cultured epithelial cells indicate that the polarized distribution of the PAR3/PAR6/aPKC complex is crucial for establishing epithelial cell polarity by regulating junctional structures. *C. elegans* PAR3 and its homolog Bazooka in *Drosophila* are essential for the development of these organisms by regulating polarity of various cell types (Macara, 2004; Ohno, 2001). Furthermore, recent evidence from an in vitro study imply the involvement of PAR3 in epithelial cyst development (Hurd et al., 2003). These observations suggest the importance of PAR3 in mammalian development through the regulation of epithelial cell polarity. However, direct evidence that reveals the significance of PAR3 in mammalian development has not yet been obtained.

Among various epithelial cell cysts, EPP cell cysts play a crucial role in mammalian cardiac morphogenesis (Manner et al., 2001). The cardiac walls consist of three different tissue layers: the epicardium, myocardium and endocardium. In particular, epicardial development is a unique process that features two different mechanisms by which epicardial cells the envelope entire heart. EPP cells differentiate from mesenchymal cells in the septum transversum through mesenchymal-to-epithelial transition and then form the proepicardial serosa on the pericardial surface of the septum transversum (Manner et al., 2001). In the first mechanism, EPP cells migrate directly from the proepicardial serosa to the dorsal surface of the developing atrium and spread as a continuous epithelial sheet. This mechanism predominates in avian embryos

(Manner, 1992). In the second mechanism, EPP cells bud out from the proepicardial serosa forming cell cysts. The EPP cell cysts float into the pericardial cavity to reach the myocardium and the cells spread from the cysts to form isolated patches of epicardial sheets (Sengbusch et al., 2002). This cyst-mediated mechanism predominates in mammals (Komiyama et al., 1987; Kuhn and Liebherr, 1988; Viragh and Challice, 1981). Finally, the epicardial sheets formed by both mechanisms coalesce to form a coherent epicardium. In addition, the epicardium plays two crucial roles in cardiac development: first, epicardial cells secrete soluble tropic factor(s) required for cardiomyocyte proliferation (Chen et al., 2002; Stuckmann et al., 2003); second, some epicardial cells subsequently develop into coronary vessels (Manner et al., 2001). Despite the fundamental roles of EPP cell cysts in mammalian cardiac development, the molecular mechanisms underlying EPP cell cyst formation are poorly understood. Targeted gene disruption in mice has revealed the important roles of the Wilms' tumor 1 (*Wt1*) tumor suppressor gene and the interaction of α4 integrin with fibronectin in the formation of EPP cell cysts: WT1 is required in the mesenchymal-to-epithelial transition of EPP cells, and the interaction of α4 integrin with fibronectin is involved in the proper EPP cell cyst formation (Moore et al., 1999; Sengbusch et al., 2002). However, any other molecules essential for EPP cell cyst formation have not been identified to date. We report here the first study, using PAR3-deficient mice, showing that PAR3 is essential for cyst-mediated epicardial development in mice. Although the EPP cell fate is determined in PAR3-deficient mice, EPP cells fail to form cysts, despite the retention of the activities of proliferation and migration to the myocardium. PAR3-deficient EPP cells show defects in the localization of PAR-6β, aPKC and ezrin to the apical domains but a normal localization of α4/β1 integrins and ZO1 to the basolateral domains and cell-cell junctions, respectively. Given the findings that cell-ECM and cell-cell interactions provide the spatial cues for epithelial cell polarity, we propose that PAR3 interprets the spatial cell polarity cues from integrins and cell-cell contacts to establish the apical cortical domains of EPP cells.

MATERIALS AND METHODS

Targeted disruption of mouse *Par3* gene

In accordance with a previous report (Shibata et al., 1997), a 129/Sv mouse genomic DNA fragment of 14.2 kb, containing the third coding exon of the *Par3* gene, was isolated. An MC1-Neo cassette, flanked by two loxP sequences, and one loxP sequence were introduced into the *Nsi*I site in intron 2 and the *Nde*I site in intron 3, respectively. An MC1-DT-A cassette was attached at the *Nco*I site in intron 2 and the targeting vector was linearized at the *Not*I site. As described previously (Shibata et al., 1997), the electroporation and G418 selection of J1 ES cells were carried out, and homologous recombinant ES cells were identified by Southern blot analysis, and injected into C57BL/6J blastocysts. Two independent chimeric mice were established from distinct ES cell clones, and the chimeric mice or their offspring were mated with CAG-cre transgenic female mice (Sakai and Miyazaki, 1997). All of the oocytes in hemizygous CAG-cre transgenic mice have cre recombinase irrespective of the cre transgene transmission and recombine the loxP-flanked genomic region carried by the sperm fertilizing with the egg (Sakai and Miyazaki, 1997). The resulting mice with the $Par3^{\Delta E3}$ allele but without the cre transgene were backcrossed to C57BL/6J mice to maintain two independent lines on a mixed 129Sv/C57BL6J background. Both lines of mice showed the consistent phenotypes. Our institutional review boards have approved all animal experimental procedures described in this manuscript.

Western blotting

The head regions of embryonic day 11.5 (E11.5) embryos in a single litter were subjected to SDS-PAGE using discontinuous acrylamide gel (8%, 15%), and the PAR3 protein was detected by western blotting with C2-3AP pAb (0.5 μg/ml) as described previously (Hirose et al., 2002). The remaining parts of the embryos were subjected to Southern blot analysis.

Histology and immunostaining

Dissected embryos were fixed in Bouin's fixative (3 hours, 4°C), dehydrated and embedded in paraffin wax. Sections were stained with Carazzi's Hematoxylin (Muto pure chemicals), Eosin and phloxine B (Sigma), and photographed under a DMR microscope (Leica) equipped with a CCD camera (Pixera).

The paraffin sections of Bouin-fixed embryos were processed for heat-induced epitope retrieval using a DAKO target retrieval solution high pH (S3308) for anti-GATA4 mAb (1.5 μg/ml, G-4, Santa Cruz) and anti-aPKCι mAb (1 μg/ml, clone 23, BD Transduction Laboratories), or DAKO target retrieval solution (S1700) for anti-WT-1 pAb (1 μg/ml, C-19, Santa Cruz), anti-BrdU mAb (0.5 μg/ml, B44, Becton Dickinson) and anti-αSMA mAb (34 ng/ml, 1A4, Zymed). Embryos fixed in paraformaldehyde-lysine-periodate fixative (2 hours, 4°C) (McLean and Nakane, 1974) were quenched in 100 mM NH_4Cl in PBS (1 hour, 4°C), processed for cryosectioning, and permeabilized and blocked with an Image-iT FX signal enhancer (Molecular Probes). The sections were blocked with 10% normal goat serum in PBS and subjected to immunohistochemistry or immunofluorescence labeling using the primary antibodies including anti-α4 integrin (5 μg/ml, 9C10, BD PharMingen; 20 μg/ml, PS/2, Chemicon), VCAM1 (1 μg/ml, MVCAM.A429, BD PharMingen), PECAM1 (0.5 μg/ml, MEC13.3, BD PharMingen), PAR3 (1 μg/ml, C2-3AP, Hirose et al., 2002; 5 μg/ml, #07-330, Upstate), PAR6β (0.5 μg/ml, BC32AP; 1 μg/ml, BCR12AP) (Yamanaka et al., 2003), aPKCλ/ζ (2.5 μg/ml, C-20, Santa Cruz), β1 integrin (2.5 μg/ml, MB1.2, Chemicon), ZO1 (2.5 μg/ml, ZO1-1A12, Zymed) and ezrin (1:500, 3C12, Sigma). Each pair of antibodies showed consistent staining for α4 integrin (9C10, PS/2), PAR3 (C2-3AP, #07-330), PAR6β (BC32AP, BCR12AP) and aPKC (clone 23, C-20). For immunohistochemistry, biotinylated secondary antibodies (2 μg/ml, anti-rat IgGs, BioSource; 1 μg/ml, anti-rabbit IgGs, Vector Laboratories) were visualized using a Vectastain Elite ABC kit (Vector Laboratories) and counterstained with Hematoxylin. For immunofluorescence labeling, the primary antibodies were visualized using biotinylated secondary antibodies (2 μg/ml, anti-rat IgGs, BioSource; 1.5 μg/ml, anti-mouse IgGs, Vector Laboratories) with fluorescein-avidin (2 μg/ml, Vector Laboratories), or using Cy3-, Cy5- (1 or 2 μg/ml, respectively, Amersham Bioscience) or Alexa647-conjugated (2.5 μg/ml, Molecular Probes) secondary antibodies. Images were captured under a BX50 fluorescence microscope (Olympus) equipped with a CCD camera (Photometrics). All images were arranged and labeled using Photoshop 5.5 (Adobe Systems).

BrdU-labeling analysis

Pregnant mice were intraperitoneally injected with BrdU (50 mg/kg) 1 hour before sacrifice. WT1- and BrdU-positive cells were detected as described above. Four to 10 sections were used to count at least 100 and 213 WT1-positive cells per embryo at E9.5 and E10.5, respectively.

Modified Boyden chamber assay

In accordance with a previous report (Sengbusch et al., 2002), the upper and bottom surfaces of TransWell filters (8 μm pores, #3422, Costar) were precoated with human plasma fibronectin (Gibco) in DMEM (10 μg/ml) for 2 hours at 37°C and the substrate in the upper compartment was removed. Proepicardial serosa explants from E9.5 embryos were placed in the upper compartments containing fibronectin-free DMEM and cultured for 24 hours at 37°C. The explants were fixed in 2% paraformaldehyde for 10 minutes; cells on the upper membrane surface were removed using a cotton swab and cells on the bottom membrane surface were stained for WT1.

RESULTS

Targeted disruption of the mouse *Par3* gene resulted in midgestational embryonic lethality

To explore the function of PAR3 in epithelial morphogenesis in vivo, we generated PAR3-deficient mice by homologous recombination in embryonic stem (ES) cells followed by Cre-mediated

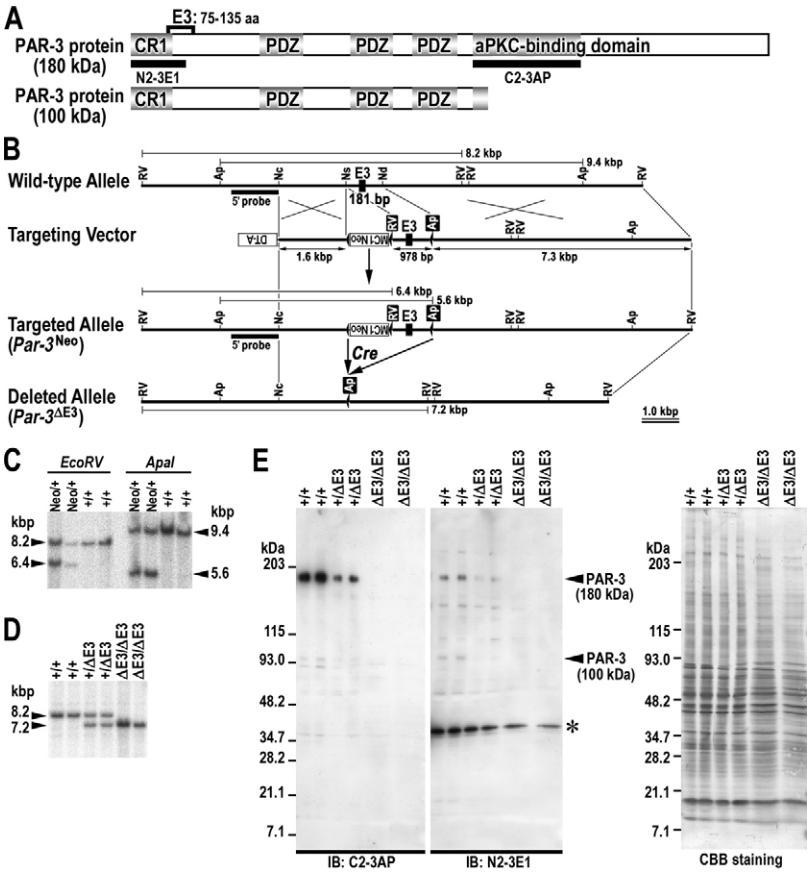

Fig. 1. Targeted disruption of mouse *Par3* gene. (**A**) Schematic structures of the full-length PAR3 protein (180 kDa) and a major splice variant (100 kDa) expressed in mouse embryos. The third exon (E3) encodes amino acids 75-135. Anti-PAR3 antibodies were raised against amino acids 1-115 (N2-3E1) or 712-936 (C2-3AP). CR1 and PDZ indicate the conserved oligomerization and PDZ domains, respectively. (**B**) Restriction maps of wild-type mouse *Par3* genomic locus, targeting vector, targeted allele ($Par3^{Neo}$) and *Par3* deleted allele ($Par3^{\Delta E3}$) obtained after cre-mediated excision of loxP-flanked region, including the third exon (E3, 181 bp, boxes), which encodes amino acids 75-135. The targeting vector has one loxP-flanked MC1-neo cassette in intron 2, one loxP site in intron 3 and one MC1-DT-A-negative selection marker. The loxP sequences are shown in triangles. The position of the 5′ external probe for Southern blot analysis is indicated. RV, *Eco*RV; Ap, *Apa*I; Nc, *Nco*I; Ns, *Nsi*I; Nd, *Nde*I. (**C**) Southern blotting of *Eco*RV- or *Apa*I-digested genomic DNA from wild-type (+/+) and heterozygous (Neo/+) littermates. The size of each band yielded by the 5′ external probe is indicated. (**D**) Southern blotting of *Eco*RV-digested genomic DNA from wild-type (+/+), heterozygous (+/ΔE3) and homozygous (ΔE3/ΔE3) littermates. The 5′ external probe yields an 8.2 kb band from the wild-type allele, and a 7.2 kb band from the $Par3^{\Delta E3}$ allele. (**E**) The loss of the PAR3 protein in embryos at E11.5 was examined by immunoblotting. Protein extracts from the heads of the embryos shown in D were probed with affinity-purified anti-PAR3 antibodies (C2-3AP, N2-3E1). An asterisk indicates nonspecific bands. The CBB staining of blotted membrane is shown as a loading control.

recombination in mice. To achieve a conditional *Par3* gene disruption and avoid the risk of expressing a truncated PAR3 protein from in-frame ATGs in downstream exons after the Cre-mediated recombination, we engineered a conditional *Par3* allele with loxP sites flanking coding exon 3 of the *Par3* gene by homologous recombination in mouse ES cells (targeted allele, $Par3^{Neo}$ in Fig. 1B,C). Two distinct mouse lines were established from independently targeted ES cell clones. The zygotic deletion of coding exon 3 was achieved by the crossing of these mouse lines with CAG-cre transgenic female mice (Sakai and Miyazaki, 1997), and the resulting offspring without the cre transgene were used in analyses (deleted allele, $Par3^{\Delta E3}$ in Fig. 1B,D). Because exon 3 consists of 181 bp, its deletion results in a frame-shift mutation at codon 75, leading to a premature termination in the CR1 domain of the PAR3 protein (Izumi et al., 1998). The CR1 domain is a conserved oligomerization domain responsible for the functions of PAR3 homologs in the *Drosophila* follicular epithelium and cultured MDCK cells (Benton and Johnston, 2003; Mizuno et al., 2003). The suppression of the PAR3 protein expression was confirmed by the immunoblotting of embryonic lysates (Fig. 1E). The use of the affinity-purified antibody against the aPKC-binding region of PAR3 revealed a single band corresponding to a protein of 180 kDa for wild-type (+/+) and heterozygous (+/ΔE3) embryos. The use of another affinity-purified antibody against the N terminus of PAR3 identified the expression of 180 kDa and 100 kDa PAR3 in wild-type (+/+) and heterozygous (+/ΔE3) embryos as reported previously (Lin et al., 2000). By contrast, the expression of both PAR3 isoforms in $Par3^{\Delta E3/\Delta E3}$ embryos was below the detection limit, indicating that the $Par3^{\Delta E3}$ allele carries a strong loss-of-function mutation.

Mice heterozygous for the *Par3* mutation ($Par3^{+/\Delta E3}$) were born from heterozygote backcrosses at the expected Mendelian ratio (n=276/542, 50.9%), were fully developed, were fertile and lacked the

Table 1. Frequencies of genotypes in progeny from heterozygote intercrosses

	Genotype			ΔE3/ΔE3 embryos				
					Growth arrest			
Stage	+/+	+/ΔE3	ΔE3/ΔE3	Grossly normal	Mild	Severe*	Deteriorated	Resorbed†
E9.5	80 (26.5%)	153 (50.7%)	69 (22.8%)	5	35	29	0	0
E10.5	47 (22.2%)	114 (53.8%)	51 (24.1%)	4	18	16	13	0
E11.5	26 (32.1%)	41 (50.6%)	14 (17.3%)	1	1	1	11	0
E12.5	4 (26.7%)	5 (33.3%)	6 (40.0%)	0	0	0	5	1
E14.5	2 (40.0%)	2 (40.0%)	1 (20.0%)	0	0	0	0	1
E18.5	6 (42.9%)	8 (57.1%)	0 (0.0%)					
Live born	72 (37.7%)	119 (62.3%)	0 (0.0%)					

*Embryos with severe growth arrest, but they still had heartbeats.
†Only yolk sacs were obtained.

overt symptoms of a disease. However, no homozygous mutants (*Par3*$^{\Delta E3/\Delta E3}$) were identified among pups born from heterozygote intercrosses (n=0/191). To determine the time of death of *Par3*$^{\Delta E3/\Delta E3}$ embryos, we analyzed embryos at different stages from E9.5 to E18.5 (Table 1). *Par3*$^{\Delta E3/\Delta E3}$ embryos at E9.5 were obtained at approximately the expected Mendelian ratio. Although all the *Par3*$^{\Delta E3/\Delta E3}$ embryos had heartbeats at E9.5, they showed developmental delay and growth retardation in various degrees. As development proceeds, growth defects in *Par3*$^{\Delta E3/\Delta E3}$ embryos became more severe and no living embryos were detected after E12.5. Thus, these data demonstrate that the disruption of the *Par3* gene leads to a recessive embryonic lethality in the midgestational stage.

Defective cardiac development in *Par3*$^{\Delta E3/\Delta E3}$ embryos

Because midgestational lethality suggests a failure in early organogenesis in *Par3*$^{\Delta E3/\Delta E3}$ embryos (Copp, 1995), we focused our analysis on organogenesis from E9.5 to E10.5. We first examined whole-mount *Par3*$^{\Delta E3/\Delta E3}$ embryos at E9.5 and E10.5. Although most of the *Par3*$^{\Delta E3/\Delta E3}$ embryos had heartbeats at E9.5, two distinct types of defect were observed among *Par3*$^{\Delta E3/\Delta E3}$ embryos. About 40% of *Par3*$^{\Delta E3/\Delta E3}$ embryos showed severe growth retardation at E9.5 (Fig. 2C) and about 25% of *Par3*$^{\Delta E3/\Delta E3}$ embryos were dead at E10.5 (Table 1). The remaining 60-75% of *Par3*$^{\Delta E3/\Delta E3}$ embryos showed mild to slight growth retardation at E9.5 (Fig. 2B) and survived up to E10.5 (Table 1). Thus, we chose only *Par3*$^{\Delta E3/\Delta E3}$ embryos without severe growth retardation in the subsequent analyses. Even *Par3*$^{\Delta E3/\Delta E3}$ embryos with slight growth retardation showed deficits in the formations of hearts, prominent telencephalic vesicles and caudal embryonic regions resulting in shorter tails (Fig. 2E). In particular, *Par3*$^{\Delta E3/\Delta E3}$ embryos at E10.5 have the hypoplastic ventricles (asterisk) and atria (arrowhead) compared with their wild-type littermates (Fig. 2D′,E′). Furthermore, severely affected *Par3*$^{\Delta E3/\Delta E3}$ embryos at E10.5 show enlarged atria and peripheral edemas (Fig. 2G), indicating a contractile failure of their hypoplastic hearts. However, such signs of a congestive cardiac failure were not found in wild-type littermates at E10.5 (Fig. 2F). Although *Par3*$^{\Delta E3/\Delta E3}$ embryos developed properly organized somite pairs, their shorter tails may suggest slight defects in somitogenesis. Otherwise, *Par3*$^{\Delta E3/\Delta E3}$ embryos developed virtually normal neural tubes, placentas and erythroblasts in the blood vessels of yolk sacs and embryonic tissues (Fig. 2I; data not shown). Thus, these observations indicate that cardiac development is severely affected in *Par3*$^{\Delta E3/\Delta E3}$ embryos, which can mainly cause midgestational embryonic lethality.

Epicardial development was selectively affected in *Par3*$^{\Delta E3/\Delta E3}$ embryos

To further investigate the defective cardiogenesis in *Par3*$^{\Delta E3/\Delta E3}$ embryos, we performed histopathological analyses of the hearts of *Par3*$^{\Delta E3/\Delta E3}$ embryos at E9.5-E11.5. The cardiac walls consist of three different tissue layers: the epicardium, myocardium and endocardium (Fig. 3A). In particular, epicardial development is unique, because it is accomplished involving two different cell groups that originate from the same primordial tissue (Manner et al., 2001). EPP cells differentiate on the pericardial surface of the septum transversum to form the proepicardial serosa (Fig. 3A, ps). In the first mechanism, EPP cells directly migrate onto the atrial surface from the proepicardial serosa (Fig. 3A, blue arrow). In the second mechanism, EPP cells bud out from the proepicardial serosa forming cell cysts, which float to reach the myocardial surface (Fig. 3A, red arrow).

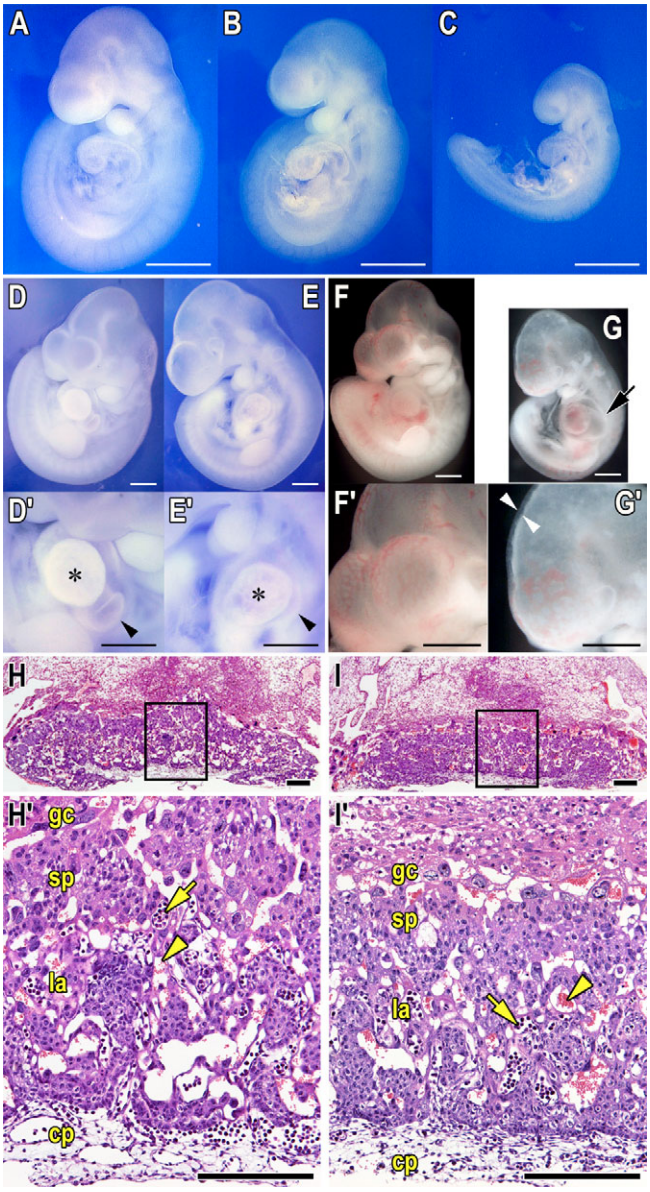

Fig. 2. *Par3*$^{\Delta E3/\Delta E3}$ embryos show growth retardation at E9.5 and cardiac defect at E10.5. (**A-G**) Gross appearance of wild-type (A,D,F) and *Par3*$^{\Delta E3/\Delta E3}$ (B,C,E,G) embryos at E9.5 (A-C) and E10.5 (D-G; enlarged, D′-G′). Mild (B) to severe (C) growth retardation is observed in *Par3*$^{\Delta E3/\Delta E3}$ embryos at E9.5. Although the common ventricular chamber (asterisk) and the common atrial chamber (arrowhead) are formed in *Par3*$^{\Delta E3/\Delta E3}$ embryo at E10.5 (E′), the heart is hypoplastic. A severely affected *Par3*$^{\Delta E3/\Delta E3}$ embryo at E10.5 (G,G′) shows an enlarged atrium (arrow) and peripheral edema (arrowheads). Scale bars: 0.5 mm. (**H**,**I**) Histological analysis of the placentas from wild-type (H) and *Par3*$^{\Delta E3/\Delta E3}$ (I) littermates at E10.5 shows no significant difference in the development of the giant cells (gc), spongiotrophoblasts (sp), labyrinth (la) and cholionic plates (cp). Both placentas show abundant embryonic blood vessels (arrows) and their close proximity to maternal blood sinuses (arrowheads). The indicated regions are enlarged in H′ and I′. Scale bars: 200 μm.

The histopathological analysis of *Par3*$^{\Delta E3/\Delta E3}$ embryos showed no obvious defects in the formation of the heart chambers, outflow tracts (Fig. 3D,F), endocardial cushions and trabeculations in the ventricles (Fig. S1 in the supplementary material). In wild-type

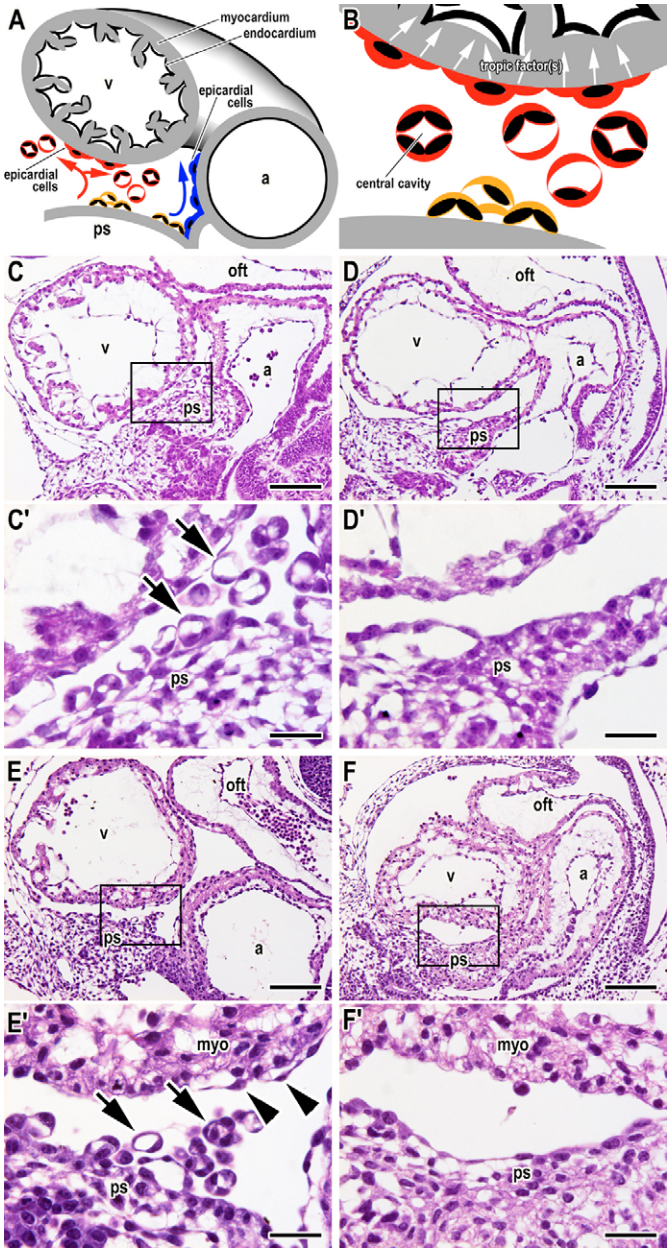

Fig. 3. Histopathological analysis reveals that *Par3*$^{\Delta E3/\Delta E3}$ embryos lack epicardial cells. (**A**,**B**) Diagrams representing epicardial development by two cellular mechanisms. (1) Red arrow: epicardial progenitor cells form cell cysts with a central cavity. The cysts bud out from the pericardial surface of the septum transversum (proepicardial serosa: ps) and float to reach the myocardial surface of the heart (v, ventricle; a, atrium), and attached epicardial cells spread to cover the heart chambers (enlarged schema in B). (2) Blue arrow: epicardial progenitor cells migrate directly to and spread over the atrial chamber as a continuous epithelial sheet. Epicardial cells secrete soluble tropic factor(s) required for cardiomyocyte proliferation (B, arrows). In all the figures, anterior is towards the left and cranial is towards the top. (**C-F**) Hematoxylin and Eosin staining of sagittal sections obtained from wild-type (C,E) and *Par3*$^{\Delta E3/\Delta E3}$ littermates (D,F) at E9.5 (C,D) or E10.5 (E,F). C′-F′ are higher magnifications of the regions shown in C-F, respectively. The specifications of the heart chambers (v, ventricle; a, atrium) and outflow tract (oft) are not affected in *Par3*$^{\Delta E3/\Delta E3}$ embryos. In wild-type embryos at E9.5 and E10.5, a substantial number of epicardial progenitor cell cysts (C′,E′, arrows) are formed and bud out from the proepicardial serosa (ps). However, no cell cysts are observed in the corresponding regions of *Par3*$^{\Delta E3/\Delta E3}$ embryos (D′,F′) at either stage. At E10.5, the myocardial surface (myo) in the wild-type ventricle, but not in the *Par3*$^{\Delta E3/\Delta E3}$ ventricle, is covered with a single layer of flat epicardial cells (E′, arrowheads). Scale bars: 100 μm for C-F; 25 μm for C′-F′.

littermates, typical EPP cell cysts were formed in the proepicardial serosa at E9.5-E10.5 (Fig. 3C′,E′, arrows) and the myocardium was covered with a single layer of flat cells at E10.5-11.5 (Fig. 3E′, arrowheads; Fig. S1 in the supplementary material), indicating normal epicardial development (Komiyama et al., 1987; Viragh and Challice, 1981). In *Par3*$^{\Delta E3/\Delta E3}$ embryos, however, typical EPP cell cysts were not detected at E9.5-E10.5 and the myocardium was not covered with a single layer of flat cells at E10.5-11.5 (Fig. 3F′; Fig. S1 in the supplementary material). Thus, we conclude that epicardial development is affected in *Par3*$^{\Delta E3/\Delta E3}$ embryos.

To assess whether epicardial development is selectively affected in *Par3*$^{\Delta E3/\Delta E3}$ hearts, we confirmed the expression of specific markers of each cardiac tissue at E9.5 (Fig. 4A-E,A′-E′). α4 integrin is a marker of EPP and epicardial cells (Sengbusch et al., 2002). GATA4 is essential for the formation of the proepicardium and regulates cardiogenesis (Watt et al., 2004). In wild-type littermates, the heart surface was covered with an α4 integrin-positive single-layer cell sheet (Fig. 4A). In addition, the proepicardial serosa and typical EPP cell cysts budding out from them were also positive for α4 integrin and GATA4 (Fig. 4A,B, arrowheads). In *Par3*$^{\Delta E3/\Delta E3}$ embryos, we detected α4 integrin- or GATA-4-positive cells in the proepicardial serosa (Fig. 4A′,B′, arrowheads), although these cells had an aberrant morphology with no cyst formation, suggesting that the epicardial cell fate is determined but cyst formation is affected. In *Par3*$^{\Delta E3/\Delta E3}$ embryos, moreover, the heart surface lacked α4 integrin-positive cells, indicating that epicardial development does not proceed normally. By contrast, wild-type littermates and *Par3*$^{\Delta E3/\Delta E3}$ embryos showed no significant difference in the expression pattern of both markers of the myocardium (VCAM1, Fig. 4C,C′; αSMA, Fig. 4D,D′) (Kwee et al., 1995; Ruzicka and Schwartz, 1988) and endocardium (PECAM1; Fig. 4E,F) (Vecchi et al., 1994). In addition, the expression pattern of GATA4 in the myocardium and endocardium was not affected in *Par3*$^{\Delta E3/\Delta E3}$ embryos (Fig. 4B′). Furthermore, the proliferation of myocardial and endocardial cells was not affected in *Par3*$^{\Delta E3/\Delta E3}$ embryos at E9.5 and E10.5 (Fig. S2 in the supplementary material). Taken together, despite the retention of the initial determination of the EPP cell fate, further epicardial development is selectively affected in *Par3*$^{\Delta E3/\Delta E3}$ embryos.

To further examine the role of PAR3 in epicardial development, we analyzed the expression of the PAR3 protein in the hearts of embryos at E9.5. In wild-type hearts (Fig. 4F), the EPP (arrows) and epicardial cells (arrowheads) expressed both α4 integrin and PAR3. PAR3 colocalized with ZO1 in these cells (Fig. 4G, arrowheads), whereas PAR3 was not detected in the cell-cell junctions in the endocardium labeled with ZO1 and PECAM1 (arrows). These observations suggest that PAR3 concentrates in the cell-cell junctions of the EPP and epicardial cells similarly to other epithelial cells (Hirose et al., 2002; Izumi et al., 1998; Manabe et al., 2002; Takaki et al., 2001). However, *Par3*$^{\Delta E3/\Delta E3}$ hearts showed no detectable signals for PAR3 (Fig. 4F′,G′). In addition, an excessively large number of α4 integrin-positive EPP cells accumulated in the *Par3*$^{\Delta E3/\Delta E3}$ proepicardial

serosa (Fig. 4F′), suggesting a defect of EPP cells in budding out from the proepicardial serosa. Thus, these observations are consistent with that of a selective defect in epicardial development in *Par3*$^{\Delta E3/\Delta E3}$ embryos.

EPP cell cyst formation, not migration and proliferation of epicardial progenitor cells, was affected in *Par3*$^{\Delta E3/\Delta E3}$ embryos

As indicated in Fig. 3A, EPP cells reach the heart via two mechanisms. To investigate the function of PAR3 in epicardial development further, the sections of paraffin-embedded embryos at E10.5 were stained for WT1, another marker of EPP and epicardial cells (Moore et al., 1999). In wild-type hearts (Fig. 5A), typical EPP cell cysts (arrow) were identified and confirmed positive for WT1. Although no EPP cell cysts were identified in *Par3*$^{\Delta E3/\Delta E3}$ embryos, WT1-positive cells were identified in the proepicardial serosa (Fig. 5B). In addition, we found WT1-positive cell layers continuing directly from the proepicardial serosa and partially covering the atria of *Par3*$^{\Delta E3/\Delta E3}$ embryos, as observed in wild-type littermates (Fig. 5A,B, arrowheads). We next assessed the proliferation activity of EPP cells by BrdU pulse labeling at E9.5 and E10.5. There was no significant difference in the proportion of BrdU-labeled EPP cells expressing WT1 between *Par3*$^{\Delta E3/\Delta E3}$ and control littermates (Fig. 5C,D), suggesting that the proliferation of *Par3*$^{\Delta E3/\Delta E3}$ EPP cells is not affected. Thus, although *Par3*$^{\Delta E3/\Delta E3}$ EPP cells fail to form typical EPP cell cysts, they appear to retain the activities of proliferation and migration to the myocardium.

To confirm the notion that *Par3*$^{\Delta E3/\Delta E3}$ EPP cells retain migration activity, this activity was evaluated by a modified Boyden chamber assay (Fig. 5E-G) (Sengbusch et al., 2002). There was no significant

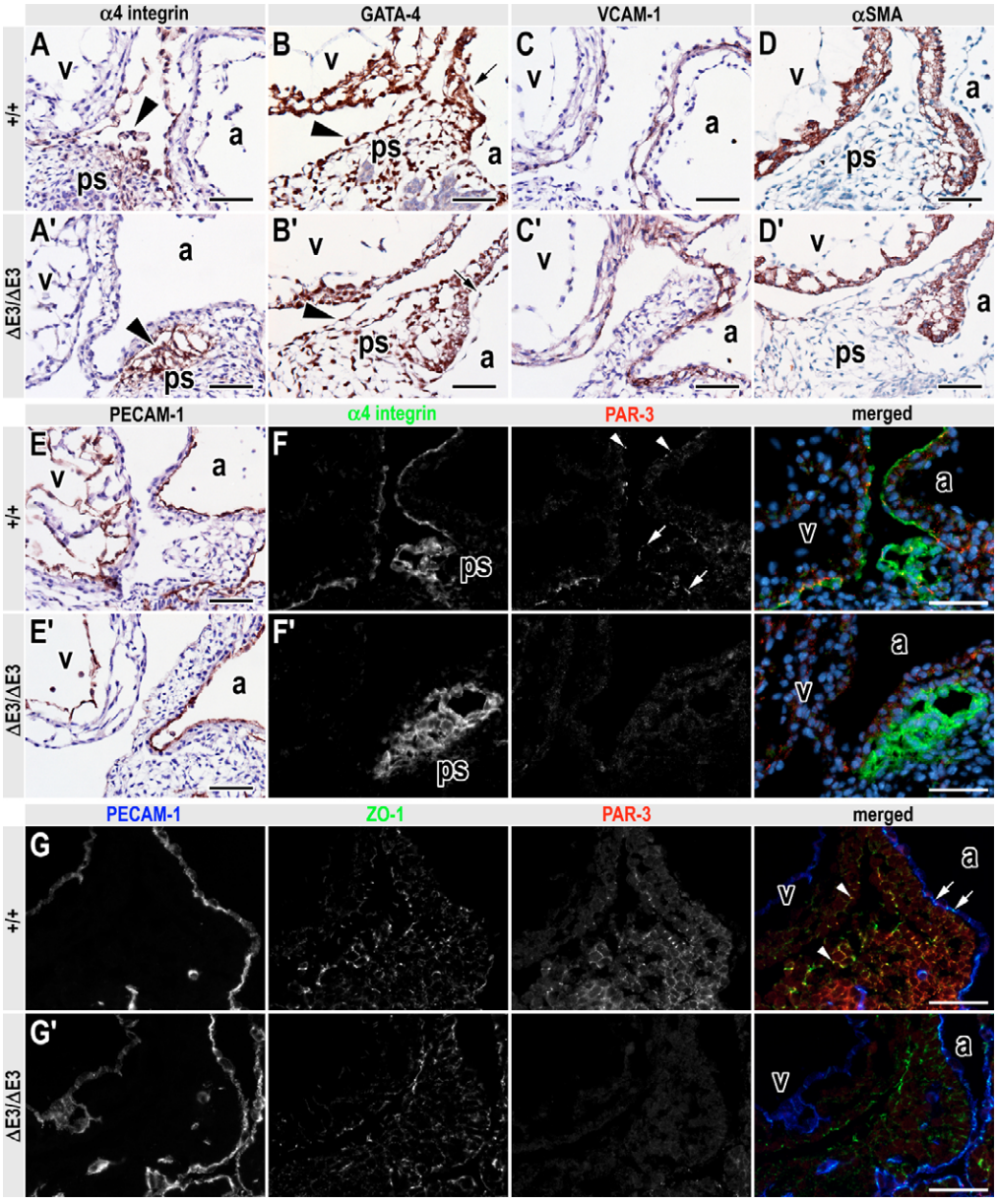

Fig. 4. Epicardial progenitor and epicardial cells are selectively affected in *Par3*$^{\Delta E3/\Delta E3}$ embryos at E9.5. (**A-E**) Immunohistochemical identification of epicardium, myocardium and endocardium using antibodies against α4 integrin (A), VCAM1 (C) or α smooth muscle actin (D; αSMA), and PECAM1 (E), respectively. All of these tissues were also labeled with anti-GATA4 mAb. The ventricle (v) and atrium (a) of a wild-type heart, but not those of a *Par3*$^{\Delta E3/\Delta E3}$ heart, are enveloped with a single layer of cells positive for α4 integrin. Although the proepicardial serosae (ps) of wild-type and *Par3*$^{\Delta E3/\Delta E3}$ hearts are positive for α4 integrin and GATA-4, the cardiac morphology is different: the *Par3*$^{\Delta E3/\Delta E3}$ heart lacks cell cysts (A′,B′, arrowheads), which are formed in the wild-type heart (A,B). The staining patterns of GATA4, VCAM1 and αSMA in the myocardium, and those for GATA4 and PECAM1 in the endocardium, are indistinguishable between wild-type and *Par3*$^{\Delta E3/\Delta E3}$ littermates. Scale bars: 50 μm. (**F**,**G**) Epicardial progenitor and epicardial cells express the PAR3 protein in the cell-cell junctions. Immunofluorescent microscopy images of α4 integrin (green), PAR3 (red), DAPI (cyan), PECAM1 (blue) and ZO1 (green) in wild-type and *Par3*$^{\Delta E3/\Delta E3}$ hearts of E9.5 littermates. The signals for PAR3 are detected in wild-type (F), but not in *Par3*$^{\Delta E3/\Delta E3}$ (G), proepicardial serosa (arrows) and epicardial cells (arrowheads). Although ZO1 colocalizes with PAR3 in the proepicardial serosa and epicardial cells (arrowheads, merged view in G), only ZO1 is detected in the endocardial cells (arrows). *Par3*$^{\Delta E3/\Delta E3}$ proepicardial serosa (F′, ps) shows an aberrant accumulation of α4 integrin-positive cells. Scale bars: 50 μm.

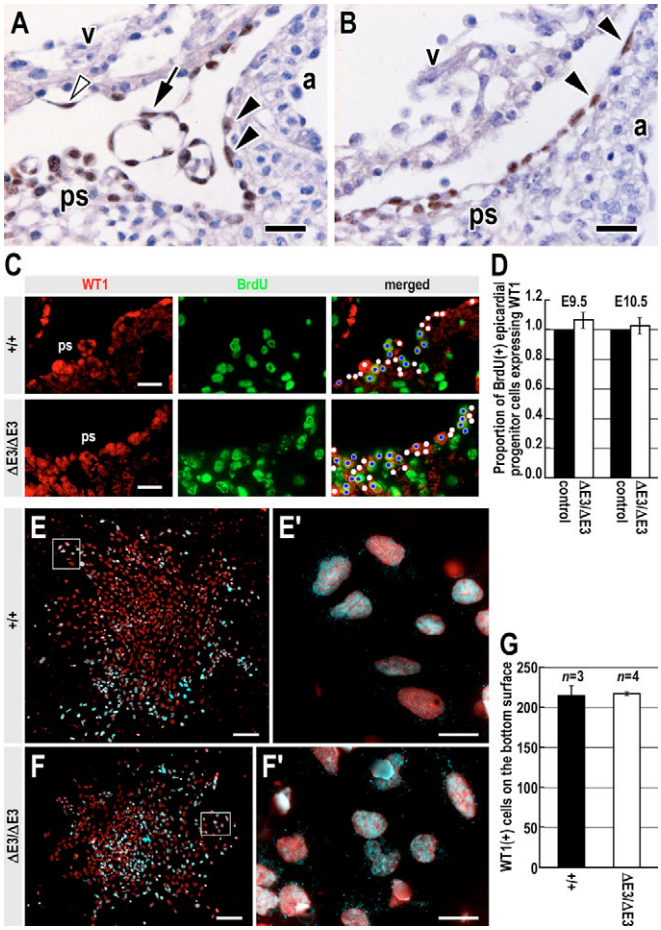

Fig. 5. The epicardial progenitor cells in *Par3*$^{\Delta E3/\Delta E3}$ embryos do not form cell cysts but retain migration and proliferation activities. (**A**,**B**) Immunohistochemistry revealed WT1 in the nuclei of epicardial progenitor cells and epicardial cells in wild-type (A) and *Par3*$^{\Delta E3/\Delta E3}$ (B) littermates at E10.5. A wild-type embryo forms typical WT1-positive EPP cell cysts (arrow), and the ventricle (v) and atrium (a) are covered with a single layer of epicardial cells (arrowheads). Although a *Par3*$^{\Delta E3/\Delta E3}$ heart has an abnormal proepicardial serosa (ps) lacking typical budding cysts, the atrium, not the ventricle, is partially covered with a single layer of epicardial cells (arrowheads). Scale bars: 20 μm. (**C**) Representative immunofluorescence images for WT1 and BrdU in wild-type and *Par3*$^{\Delta E3/\Delta E3}$ proepicardial serosae (ps) pulse-labeled for 1 hour with BrdU at E10.5. The BrdU-positive (blue spots) and -negative (white spots) epicardial progenitor cells expressing WT1 were counted in three pairs of *Par3*$^{\Delta E3/\Delta E3}$ and control littermates at E9.5 and E10.5. Scale bars: 20 μm. (**D**) The proportion of BrdU-positive epicardial progenitor cells shows no significant difference between *Par3*$^{\Delta E3/\Delta E3}$ and control littermates at E9.5 and E10.5. The proportion of the BrdU-positive cells with respect to the corresponding control littermates is considered as 1.0 and values shown are mean±s.d of three independent pairs of littermates. (**E**,**F**) Modified Boyden chamber assay on epicardial explant cells from wild-type and *Par3*$^{\Delta E3/\Delta E3}$ embryos at E9.5. After a 24-hour incubation, cells that remained on the upper surface were removed and the epicardial progenitor cells migrated to the bottom surface were identified by staining for WT1 (cyan) and DNA (red). (E′,F′) High-magnification views of the regions shown in E,F, respectively. Scale bars: 100 μm for E,F; 20 μm for E′,F′. (**G**) The quantification of the number of WT1-positive epicardial progenitor cells in modified Boyden chamber assay shows no significant difference in the migration between wild-type and *Par3*$^{\Delta E3/\Delta E3}$ epicardial progenitor cells. The explants from three wild-type and four *Par3*$^{\Delta E3/\Delta E3}$ embryos were analyzed. Error bars represent s.e.m.

difference in the number of migrated EPP cells between wild-type and *Par3*$^{\Delta E3/\Delta E3}$ EPP cells (Fig. 5G). Taken together with the observation of WT1-positive cells in *Par3*$^{\Delta E3/\Delta E3}$ embryos, these observations suggest that PAR3 is responsible for the cyst-mediated, but not direct migration-mediated, development of the epicardium.

The organization of apical cortical domains was disturbed in *Par3*$^{\Delta E3/\Delta E3}$ EPP cells

EPP cell cyst formation is selectively affected in *Par3*$^{\Delta E3/\Delta E3}$ embryos. It is crucial for the development of coherent epithelial cell cysts to establish cell-cell junctions and the polarized compartmentation of cortical subdomains; the apical domain facing the lumen and the basolateral domain adhering to ECM (O'Brien et al., 2002). To further analyze the etiology of defective EPP cell cyst formation in *Par3*$^{\Delta E3/\Delta E3}$ embryos, we assessed the subcellular localizations of the markers of cortical subdomains and cell-cell junctions. First, we examined the apical protein localization. In wild-type EPP cells, PAR6β and aPKC showed an apical cortical association as observed in other epithelial cells (Fig. 6A′,B′,E,G, white arrowheads) (Verstovsek et al., 1998; Yamanaka et al., 2003). In *Par3*$^{\Delta E3/\Delta E3}$ EPP cells, however, both PAR-6β and aPKC were generally mislocalized into the cytoplasm (Fig. 6C′,D′,F,H, white arrowheads). Furthermore, the apical cortical localization of ezrin in wild-type EPP cells (Saotome et al., 2004) was hardly observed in *Par3*$^{\Delta E3/\Delta E3}$ EPP cells (Fig. 6I,J, arrowheads). By contrast, both wild-type and *Par3*$^{\Delta E3/\Delta E3}$ EPP cells at E10.5 showed the same short linear or punctate pattern of ZO1 staining at cell-cell contact sites (Fig. 6E-H, black arrowheads) (Stevenson et al., 1986), indicating the establishment of cell-cell junctions in both wild-type and *Par3*$^{\Delta E3/\Delta E3}$ EPP cells as shown previously (Komiyama et al., 1987; Viragh and Challice, 1981). Last, we investigated the basal protein localization. Both α4 and β1 integrins localized to the basal domains of both wild-type and *Par3*$^{\Delta E3/\Delta E3}$ EPP cells (Fig. 6E-J, arrows). The margins of the basal domains were positive for ZO1 in both wild-type and *Par3*$^{\Delta E3/\Delta E3}$ EPP cells (Fig. 6E-H, black arrowheads). Thus, PAR3 is crucial for the apical cortical localization of PAR6β, aPKC and ezrin, but is dispensable for the basal localization of α4/β1 integrins and the cell-cell localization of ZO1. Taken together, we conclude that PAR3 plays an essential role in cyst-mediated epicardial development by establishing apical cortical domains.

DISCUSSION

Cell cysts composed of polarized epithelial cells play fundamental roles in embryonic development in mammals. For epithelial cell polarization, cell-cell contacts and integrin-mediated contacts to ECM provide spatial cues (Drubin and Nelson, 1996; Li et al., 2003; Rodriguez-Boulan and Nelson, 1989). The precise molecular mechanisms that interpret these cues for the establishment of polarized apical and basolateral plasma membrane domains remain unclarified. The PAR3/aPKC/PAR6 complex is involved in the regulation of the plasma membrane domain compartmentation of one-cell zygotes in *C. elegans*, neuronal and epithelial cells in *Drosophila* embryos, and cultured mammalian cells (Macara, 2004; Ohno, 2001). We provide here the first evidence that PAR3 plays crucial roles in the development of mouse embryos by establishing epithelial cell polarity. Our results suggest that PAR3 is essential for the establishment of apical cortical domains, but is dispensable for that of basolateral domains and the formation of cell-cell junctions in EPP cells.

A deficiency in PAR3 in mice leads to a defective cardiac development and the following observations support that this defect can cause midgestational embryonic lethality. First, the

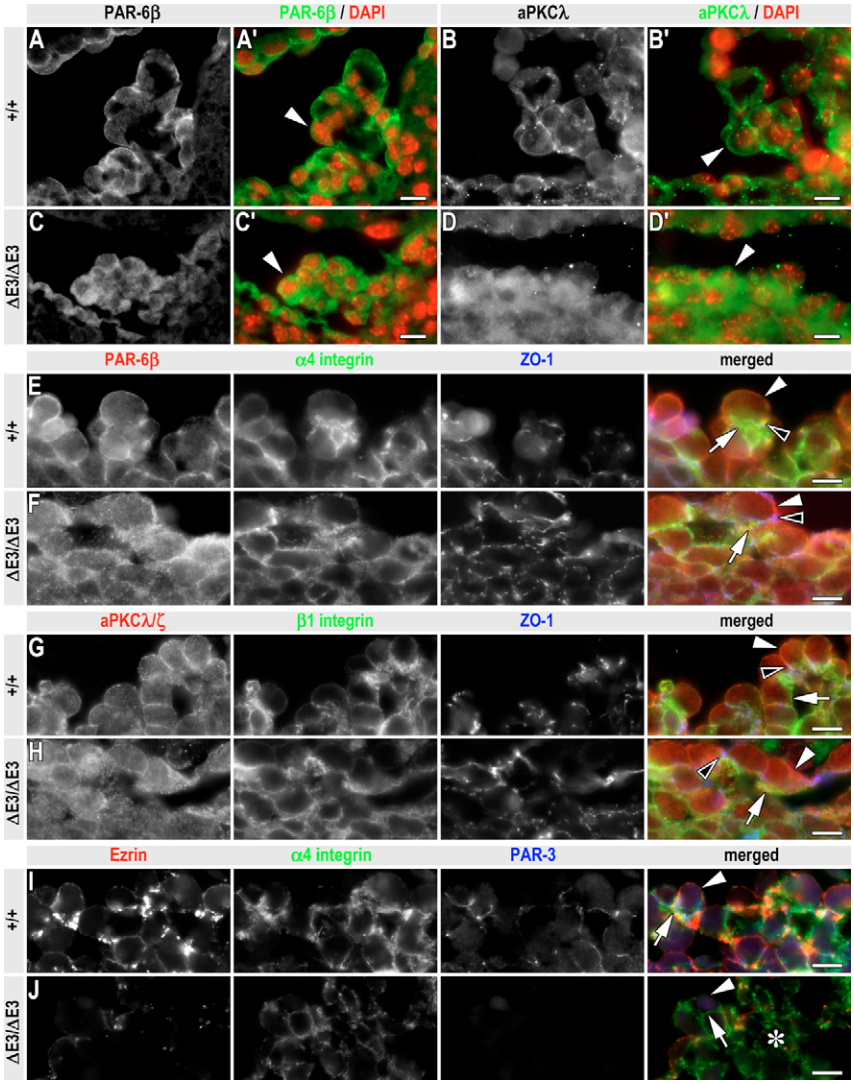

Fig. 6. PAR6β, aPKC and ezrin lose apical cortical association in *Par3*$^{\Delta E3/\Delta E3}$ epicardial progenitor cells at E10.5. (**A-D**) Although PAR6β and aPKCλ closely associate with the apical cortical domains in wild-type EPP cells, they show diffuse distribution in the EPP cells of *Par3*$^{\Delta E3/\Delta E3}$ littermates (arrowheads). DNA was stained with DAPI (red in A′-D′). Scale bars: 10 μm. (**E-J**) Localization of PAR6β, α4 integrin, ZO1, aPKCλ/ζ, β1 integrin, ezrin and PAR3 in cryosections of the EPP cells in wild-type and *Par3*$^{\Delta E3/\Delta E3}$ littermates at E10.5. Merged images are shown in the fourth column: PAR-6β, aPKCλ/ζ or ezrin, red; α4 or β1 integrin, green; ZO1 or PAR3, blue. The apical cortical association of PAR6β and aPKCλ/ζ in wild-type EPP cells is disturbed with the proteins diffusely distributed in the cytoplasm in *Par3*$^{\Delta E3/\Delta E3}$ EPP cells (E-H, white arrowheads). However, both the wild-type and *Par3*$^{\Delta E3/\Delta E3}$ EPP cells show the accumulation of α4 and β1 integrins in the basal subdomains (E-J, arrows), and ZO1 concentrates immediately apical to α4 or β1 integrins (E-H, black arrowheads). The apical cortical association of ezrin in wild-type EPP cells is mostly lost in *Par3*$^{\Delta E3/\Delta E3}$ EPP cells (I,J, arrowheads). The asterisk in J indicates an aberrant accumulation of *Par3*$^{\Delta E3/\Delta E3}$ EPP cells in the proepicardial serosa. Scale bars: 10 μm.

histopathological and immunohistological studies showed that *Par3*$^{\Delta E3/\Delta E3}$ embryos lack the epicardium (Figs 3, 4). Second, epicardial cells secrete soluble tropic factor(s) required for cardiomyocyte proliferation (Chen et al., 2002; Stuckmann et al., 2003). Consistently, *Par3*$^{\Delta E3/\Delta E3}$ hearts at E10.5 are hypoplastic (Fig. 2) and *Par3*$^{\Delta E3/\Delta E3}$ embryos at E11.5 have thin atrial walls (see Fig. S1 in the supplementary material) as observed in other mutant mice showing defective epicardial development (Kwee et al., 1995; Moore et al., 1999; Watt et al., 2004). Then what is the ontogeny of defective epicardial development in *Par3*$^{\Delta E3/\Delta E3}$ embryos? Our observations suggest that EPP cell cyst formation is defective in *Par3*$^{\Delta E3/\Delta E3}$ embryos. The EPP cell cysts are responsible for epicardial development in mammals (Manner et al., 2001). Although EPP cells were detected in *Par3*$^{\Delta E3/\Delta E3}$ embryos and proliferated normally, EPP cell cysts were not detected in *Par3*$^{\Delta E3/\Delta E3}$ embryos (Figs 3-5). The accumulation of an excessively large number of EPP cells in the proepicardial serosa in *Par3*$^{\Delta E3/\Delta E3}$ embryos may underlie the defect of EPP cells in forming cysts and budding out from the proepicardial serosa (Fig. 4). Furthermore, the disturbance in the polarity of *Par3*$^{\Delta E3/\Delta E3}$ EPP cells strongly suggests a defective development of EPP cell cysts (Fig. 6), because the organization of epithelial cell polarity is crucial for cyst formation (O'Brien et al., 2002). By contrast, the attachment of EPP cells to the heart would not be affected in *Par3*$^{\Delta E3/\Delta E3}$ embryos, because the interaction between α4 integrin and VCAM1 is sufficient for the attachment of EPP cell cysts to the heart surface (Kwee et al., 1995; Sengbusch et al., 2002) and both proteins are expressed in the developing *Par3*$^{\Delta E3/\Delta E3}$ hearts (Fig. 3). Indeed, we confirmed that *Par3*$^{\Delta E3/\Delta E3}$ EPP cells retain the α4 integrin-dependent attachment and migration activities in vivo and in vitro (Fig. 5). Nonetheless, all of the *Par3*$^{\Delta E3/\Delta E3}$ embryos fail to develop the epicardium and suffer from cardiac dysfunctions.

Although PAR3 is expressed in all of the epithelial cells investigated (Hirose et al., 2002; Izumi et al., 1998; Manabe et al., 2002; Takaki et al., 2001), we found that not all of these cells are affected in *Par3*$^{\Delta E3/\Delta E3}$ embryos. One possible explanation is the functional redundancy by the PAR3-related protein PAR3L/PAR3β (Gao et al., 2002; Kohjima et al., 2002). It has been shown that PAR3L/PAR3β colocalizes with ZO1 to cell-cell junctions (Kohjima et al., 2002) and in vitro translated PAR3L/PAR3β can associate with PAR6β in the same way as PAR3 can (Gao et al., 2002). Indeed, we found the normal localization of PAR6β in various *Par3*$^{\Delta E3/\Delta E3}$ epithelial cells, which are not affected morphologically (data not shown). By contrast, the development of the EPP cell cysts and mesonephric vesicles is affected in *Par3*$^{\Delta E3/\Delta E3}$ embryos with a mislocalization of PAR6β (Fig. 6; see Fig. S3 in the supplementary

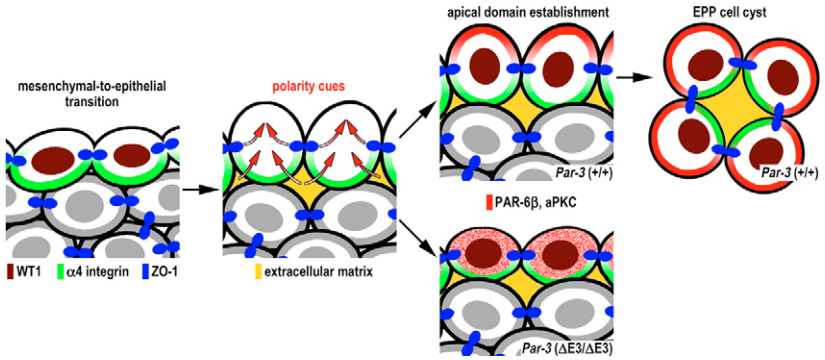

Fig. 7. Model for EPP cell cyst formation. Mesenchymal-to-epithelial transition specifies EPP cells expressing WT1 and α4 integrin. Cell-cell contacts and integrin-mediated contacts to the extracellular matrix provide spatial cues for epithelial cell polarity. PAR3 interprets the spatial cell polarity cues to localize PAR6β and aPKC, leading to the establishment of apical cortical domains of EPP cells. Completely polarized EPP cells can then form EPP cell cysts. By contrast, *Par3*$^{\Delta E3/\Delta E3}$ EPP cells fail to localize PAR6β and aPKC, and cannot establish the apical domains.

material). Taken together with the observation that mammalian PAR6 is required for epithelial cell polarity in vitro (Macara, 2004; Ohno, 2001), these observations raise a possibility that among various epithelial tissues, the polarity of EPP cell cysts and mesonephric vesicles depends on PAR3 to localize PAR6β to the apical cortical domains.

Although we did not observe an apparent mislocalization of ZO1 in cell-cell junctions in the *Par3*$^{\Delta E3/\Delta E3}$ epithelium, we found defects in the morphogenesis of epithelial tissues that originate from mesenchymal tissues via mesenchymal-to-epithelial transition: that is, EPP cell cysts and mesonephric vesicles (see Fig. S3 in the supplementary material). The morphogenesis of these two tissues requires a dynamic regulation of epithelial cell polarity and a remodeling of cell-cell and cell-ECM interactions. During a dynamic epithelial cell polarization in vitro, ZO1 localizes to immature cell-cell junctions, whereas PAR3 is recruited into the junctional complex later than ZO1 (Suzuki et al., 2002). Accumulating evidence from studies using cultured epithelial cells indicates that the PAR3/PAR6/aPKC complex is required in epithelial cell polarization by regulating the maturation of junctional structures (Hirose et al., 2002; Suzuki et al., 2001; Yamanaka et al., 2003). Our results are consistent with these observations and imply that PAR3 is essential for the dynamic remodeling of cell-cell junctions that leads to the establishment of epithelial cell polarity of EPP cell cysts and mesonephric vesicles.

Our results indicate that PAR3 is crucial for EPP cell cyst formation in the proepicardial serosa by regulating plasma membrane polarity. We also found that mesonephric vesicle formation is defective in *Par3*$^{\Delta E3/\Delta E3}$ embryos with a multilayered epithelium and disorganized lumens (see Fig. S3 in the supplementary material). Considering the finding that the accomplishment of epithelial cell polarization requires multiple steps starting from cell-cell and cell-ECM contacts (Drubin and Nelson, 1996; Gumbiner, 1996; Li et al., 2003; Rodriguez-Boulan and Nelson, 1989), we propose a simple model in which PAR3 interprets polarity cues provided by cell-cell and cell-ECM interactions leading to the establishment of apical cortical domains (Fig. 7). This model is based on the following observations. First, the expression of WT1, GATA4 and α4 integrin is retained in *Par3*$^{\Delta E3/\Delta E3}$ EPP cells (Figs 4, 5), indicating PAR3 is dispensable for mesenchymal-to-epithelial transition that specifies the EPP cell fate. Second, the normal localization of ZO1, α4 integrin and β1 integrin in *Par3*$^{\Delta E3/\Delta E3}$ EPP cells suggest that the cell-cell and cell-ECM interactions can provide polarity cues without PAR3 (Fig. 6). Furthermore, the α4 integrin-dependent cell migration activity is retained in *Par3*$^{\Delta E3/\Delta E3}$ EPP cells (Fig. 5) (Sengbusch et al., 2002), indicating that signals through α4 integrin is functional in *Par3*$^{\Delta E3/\Delta E3}$ EPP cells. Last, PAR3 plays a crucial role in the localization of PAR6β, aPKC and ezrin to the apical cortical domains of EPP cells (Fig. 6). Ezrin performs an essential function in organizing the apical cortical domains of the developing small intestinal epithelium in mice (Saotome et al., 2004). In addition, several lines of evidence imply that it is crucial for the formation of MDCK epithelial cysts to regulate epithelial cell polarity via the PAR3/aPKC/PAR6 complex and its downstream CRB3/PALS1/PATJ complex in the apical cortical domains (Hurd et al., 2003; Lemmers et al., 2004; Roh et al., 2003). Our model is further supported by the observation that *par3* RNAi in *C. elegans* disturbs the apical organization of distal spermathecal cells (Aono et al., 2004). Taken together, our present data suggest that PAR3 is responsible for epithelial cyst formations by interpreting polarity cues from the cell-cell and cell-ECM interactions that lead to the establishment of apical cortical domains.

We thank Dr J. Miyazaki for providing CAG-cre transgenic mice; H. Yamanaka, S. Kawashima, M. Fukuda, Y. Kida, C. Nakaya and A. Kawaguchi for assistance in establishing and maintaining mouse lines; and all the members of Noda and Ohno laboratories for stimulating discussions and helpful comments. T.H. was supported by the Yokohama City University Center of Excellence Program of the Ministry of Education, Culture, Sports, Science and Technology of Japan. This work was supported in part by grants from the Japan Society for the Promotion of Science (S.O.), from the Ministry of Education, Culture, Sports, Science and Technology of Japan (S.O. and T.N.), from the Collaboration of Regional Entities for the Advancement of Technological Excellence Program of the Japan Science and Technology Agency (S.O.), and from Core Research for Evolutional Science and Technology of Japan Science and Technology Agency (T.N.).

Supplementary material

Supplementary material for this article is available at
http://dev.biologists.org/cgi/content/full/133/7/1389/DC1

References

Aono, S., Legouis, R., Hoose, W. A. and Kemphues, K. J. (2004). PAR-3 is required for epithelial cell polarity in the distal spermatheca of C. elegans. *Development* **131**, 2865-2874.

Benton, R. and Johnston, D. S. (2003). A conserved oligomerization domain in drosophila Bazooka/PAR-3 is important for apical localization and epithelial polarity. *Curr. Biol.* **13**, 1330-1334.

Chen, T. H., Chang, T. C., Kang, J. O., Choudhary, B., Makita, T., Tran, C. M., Burch, J. B., Eid, H. and Sucov, H. M. (2002). Epicardial induction of fetal cardiomyocyte proliferation via a retinoic acid-inducible trophic factor. *Dev. Biol.* **250**, 198-207.

Copp, A. J. (1995). Death before birth: clues from gene knockouts and mutations. *Trends Genet.* **11**, 87-93.

Drubin, D. G. and Nelson, W. J. (1996). Origins of cell polarity. *Cell* **84**, 335-344.

Gao, L., Macara, I. G. and Joberty, G. (2002). Multiple splice variants of Par3 and of a novel related gene, Par3L, produce proteins with different binding properties. *Gene* **294**, 99-107.

Gumbiner, B. M. (1996). Cell adhesion: the molecular basis of tissue architecture and morphogenesis. *Cell* **84**, 345-357.

Hirose, T., Izumi, Y., Nagashima, Y., Tamai-Nagai, Y., Kurihara, H., Sakai, T., Suzuki, Y., Yamanaka, T., Suzuki, A., Mizuno, K. et al. (2002). Involvement of ASIP/PAR-3 in the promotion of epithelial tight junction formation. *J. Cell Sci.* **115**, 2485-2495.

Hurd, T. W., Fan, S., Liu, C. J., Kweon, H. K., Hakansson, K. and Margolis, B.

(2003). Phosphorylation-dependent binding of 14-3-3 to the polarity protein par3 regulates cell polarity in Mammalian epithelia. *Curr. Biol.* **13**, 2082-2090.
Izumi, Y., Hirose, T., Tamai, Y., Hirai, S., Nagashima, Y., Fujimoto, T., Tabuse, Y., Kemphues, K. J. and Ohno, S. (1998). An atypical PKC directly associates and colocalizes at the epithelial tight junction with ASIP, a mammalian homologue of Caenorhabditis elegans polarity protein PAR-3. *J. Cell Biol.* **143**, 95-106.
Joberty, G., Petersen, C., Gao, L. and Macara, I. G. (2000). The cell-polarity protein Par6 links Par3 and atypical protein kinase C to Cdc42. *Nat. Cell Biol.* **2**, 531-539.
Kohjima, M., Noda, Y., Takeya, R., Saito, N., Takeuchi, K. and Sumimoto, H. (2002). PAR3beta, a novel homologue of the cell polarity protein PAR3, localizes to tight junctions. *Biochem. Biophys. Res. Commun.* **299**, 641-646.
Komiyama, M., Ito, K. and Shimada, Y. (1987). Origin and development of the epicardium in the mouse embryo. *Anat. Embryol.* **176**, 183-189.
Kuhn, H. J. and Liebherr, G. (1988). The early development of the epicardium in Tupaia belangeri. *Anat. Embryol.* **177**, 225-234.
Kwee, L., Baldwin, H. S., Shen, H. M., Stewart, C. L., Buck, C., Buck, C. A. and Labow, M. A. (1995). Defective development of the embryonic and extraembryonic circulatory systems in vascular cell adhesion molecule (VCAM-1) deficient mice. *Development* **121**, 489-503.
Lemmers, C., Michel, D., Lane-Guermonprez, L., Delgrossi, M. H., Medina, E., Arsanto, J. P. and Le Bivic, A. (2004). CRB3 binds directly to Par6 and regulates the morphogenesis of the tight junctions in mammalian epithelial cells. *Mol. Biol. Cell* **15**, 1324-1333.
Li, S., Edgar, D., Fassler, R., Wadsworth, W. and Yurchenco, P. D. (2003). The role of laminin in embryonic cell polarization and tissue organization. *Dev. Cell* **4**, 613-624.
Lin, D., Edwards, A. S., Fawcett, J. P., Mbamalu, G., Scott, J. D. and Pawson, T. (2000). A mammalian PAR-3-PAR-6 complex implicated in Cdc42/Rac1 and aPKC signalling and cell polarity. *Nat. Cell Biol.* **2**, 540-547.
Macara, I. G. (2004). Parsing the polarity code. *Nat. Rev. Mol. Cell Biol.* **5**, 220-231.
Manabe, N., Hirai, S., Imai, F., Nakanishi, H., Takai, Y. and Ohno, S. (2002). Association of ASIP/mPAR-3 with adherens junctions of mouse neuroepithelial cells. *Dev. Dyn.* **225**, 61-69.
Manner, J. (1992). The development of pericardial villi in the chick embryo. *Anat. Embryol.* **186**, 379-385.
Manner, J., Perez-Pomares, J. M., Macias, D. and Munoz-Chapuli, R. (2001). The origin, formation and developmental significance of the epicardium: a review. *Cells Tissues Organs* **169**, 89-103.
McLean, I. W. and Nakane, P. K. (1974). Periodate-lysine-paraformaldehyde fixative. A new fixation for immunoelectron microscopy. *J. Histochem. Cytochem.* **22**, 1077-1083.
Mizuno, K., Suzuki, A., Hirose, T., Kitamura, K., Kutsuzawa, K., Futaki, M., Amano, Y. and Ohno, S. (2003). Self-association of PAR-3-mediated by the conserved N-terminal domain contributes to the development of epithelial tight junctions. *J. Biol. Chem.* **278**, 31240-31250.
Moore, A. W., McInnes, L., Kreidberg, J., Hastie, N. D. and Schedl, A. (1999). YAC complementation shows a requirement for Wt1 in the development of epicardium, adrenal gland and throughout nephrogenesis. *Development* **126**, 1845-1857.
O'Brien, L. E., Jou, T. S., Pollack, A. L., Zhang, Q., Hansen, S. H., Yurchenco, P. and Mostov, K. E. (2001). Rac1 orientates epithelial apical polarity through effects on basolateral laminin assembly. *Nat.Cell Biol.* **3**, 831-838.
O'Brien, L. E., Zegers, M. M. and Mostov, K. E. (2002). Opinion: building epithelial architecture: insights from three-dimensional culture models. *Nat. Rev. Mol. Cell Biol.* **3**, 531-537.
Ohno, S. (2001). Intercellular junctions and cellular polarity: the PAR-aPKC complex, a conserved core cassette playing fundamental roles in cell polarity. *Curr. Opin. Cell Biol.* **13**, 641-648.
Rodriguez-Boulan, E. and Nelson, W. J. (1989). Morphogenesis of the polarized epithelial cell phenotype. *Science* **245**, 718-725.
Roh, M. H., Fan, S., Liu, C. J. and Margolis, B. (2003). The Crumbs3-Pals1 complex participates in the establishment of polarity in mammalian epithelial cells. *J. Cell Sci.* **116**, 2895-2906.
Ruzicka, D. L. and Schwartz, R. J. (1988). Sequential activation of alpha-actin genes during avian cardiogenesis: vascular smooth muscle alpha-actin gene transcripts mark the onset of cardiomyocyte differentiation. *J. Cell Biol.* **107**, 2575-2586.
Sakai, K. and Miyazaki, J. (1997). A transgenic mouse line that retains Cre recombinase activity in mature oocytes irrespective of the cre transgene transmission. *Biochem. Biophys. Res. Commun.* **237**, 318-324.
Sakai, T., Li, S., Docheva, D., Grashoff, C., Sakai, K., Kostka, G., Braun, A., Pfeifer, A., Yurchenco, P. D. and Fassler, R. (2003). Integrin-linked kinase (ILK) is required for polarizing the epiblast, cell adhesion, and controlling actin accumulation. *Genes Dev.* **17**, 926-940.
Saotome, I., Curto, M. and McClatchey, A. I. (2004). Ezrin is essential for epithelial organization and villus morphogenesis in the developing intestine. *Dev. Cell* **6**, 855-864.
Sengbusch, J. K., He, W., Pinco, K. A. and Yang, J. T. (2002). Dual functions of [alpha]4[beta]1 integrin in epicardial development: initial migration and long-term attachment. *J. Cell Biol.* **157**, 873-882.
Shibata, H., Toyama, K., Shioya, H., Ito, M., Hirota, M., Hasegawa, S., Matsumoto, H., Takano, H., Akiyama, T., Toyoshima, K. et al. (1997). Rapid colorectal adenoma formation initiated by conditional targeting of the Apc gene. *Science* **278**, 120-123.
Stevenson, B. R., Siliciano, J. D., Mooseker, M. S. and Goodenough, D. A. (1986). Identification of ZO-1: a high molecular weight polypeptide associated with the tight junction (zonula occludens) in a variety of epithelia. *J. Cell Biol.* **103**, 755-766.
Stuckmann, I., Evans, S. and Lassar, A. B. (2003). Erythropoietin and retinoic acid, secreted from the epicardium, are required for cardiac myocyte proliferation. *Dev. Biol.* **255**, 334-349.
Suzuki, A., Yamanaka, T., Hirose, T., Manabe, N., Mizuno, K., Shimizu, M., Akimoto, K., Izumi, Y., Ohnishi, T. and Ohno, S. (2001). Atypical protein kinase C is involved in the evolutionarily conserved par protein complex and plays a critical role in establishing epithelia-specific junctional structures. *J. Cell Biol.* **152**, 1183-1196.
Suzuki, A., Ishiyama, C., Hashiba, K., Shimizu, M., Ebnet, K. and Ohno, S. (2002). aPKC kinase activity is required for the asymmetric differentiation of the premature junctional complex during epithelial cell polarization. *J. Cell Sci.* **115**, 3565-3573.
Takaki, Y., Hirai, S., Manabe, N., Izumi, Y., Hirose, T., Nakaya, M., Suzuki, A., Mizuno, K., Akimoto, K., Tsukita, S. et al. (2001). Dynamic changes in protein components of the tight junction during liver regeneration. *Cell Tissue Res.* **305**, 399-409.
Vecchi, A., Garlanda, C., Lampugnani, M. G., Resnati, M., Matteucci, C., Stoppacciaro, A., Schnurch, H., Risau, W., Ruco, L., Mantovani, A. et al. (1994). Monoclonal antibodies specific for endothelial cells of mouse blood vessels. Their application in the identification of adult and embryonic endothelium. *Eur. J. Cell Biol.* **63**, 247-254.
Verstovsek, G., Byrd, A., Frey, M. R., Petrelli, N. J. and Black, J. D. (1998). Colonocyte differentiation is associated with increased expression and altered distribution of protein kinase C isozymes. *Gastroenterology* **115**, 75-85.
Viragh, S. and Challice, C. E. (1981). The origin of the epicardium and the embryonic myocardial circulation in the mouse. *Anat. Rec.* **201**, 157-168.
Watt, A. J., Battle, M. A., Li, J. and Duncan, S. A. (2004). GATA4 is essential for formation of the proepicardium and regulates cardiogenesis. *Proc. Natl. Acad. Sci. USA* **101**, 12573-12578.
Yamanaka, T., Horikoshi, Y., Sugiyama, Y., Ishiyama, C., Suzuki, A., Hirose, T., Iwamatsu, A., Shinohara, A. and Ohno, S. (2003). Mammalian Lgl forms a protein complex with PAR-6 and aPKC independently of PAR-3 to regulate epithelial cell polarity. *Curr. Biol.* **13**, 734-743.